Theory of Localized Synfire Chain: Characteristic Propagation Speed of Stable Spike Patterns

Kosuke Hamaguchi
RIKEN Brain Science Institute
Wako, Saitama 351-0198, JAPAN
hammer@brain.riken.jp

Masato Okada
Dept. of Complexity Science and Engineering, University of Tokyo,
Kashiwa, Chiba, 277-8561, JAPAN
okada@brain.riken.jp

Kazuyuki Aihara
Institute of Industrial Science, University of Tokyo &
ERATO Aihara Complexity Modeling Project JST
Meguro, Tokyo 153-8505, JAPAN
aihara@sat.t.u-tokyo.ac.jp

Abstract

Repeated spike patterns have often been taken as evidence for the synfire chain, a phenomenon that a stable spike synchrony propagates through a feedforward network. Inter-spike intervals which represent a repeated spike pattern are influenced by the propagation speed of a spike packet. However, the relation between the propagation speed and network structure is not well understood. While it is apparent that the propagation speed depends on the excitatory synapse strength, it might also be related to spike patterns. We analyze a feedforward network with Mexican-Hat-type connectivity (FMH) using the Fokker-Planck equation. We show that both a uniform and a localized spike packet are stable in the FMH in a certain parameter region. We also demonstrate that the propagation speed depends on the distinct firing patterns in the same network.

1 Introduction

Neurons transmit information through spikes, but how the information is encoded remains a matter of debate. The classical view is that the firing rates of neurons encode information, while a recent view is that spatio-temporal spike patterns encode the information. For example, the synchrony of spikes observed in the cortex is thought to play functional roles in cognitive functions [1]. The mechanism of synchrony has been studied theoretically for several neural network models. Especially, the model of spike synchrony propagation through a feedforward network is called the *synfire chain* [2].

The mechanism of generating synchrony in a feedforward network can be described as follows. When feedforward connections are homogeneous with excitatory efficacy as a whole,

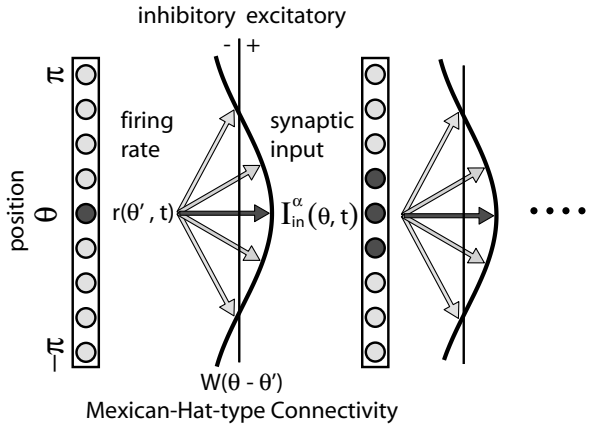

Figure 1: Network architecture. Each layer consists of N neuron arranged in a circle. Each neuron projects its axon to a post-synaptic layer with Mexican-Hat-type connectivity.

post-synaptic neurons accept similar synaptic inputs. If neurons receive similar temporally modulated inputs, the resultant spike timings will be also similar, or roughly synchronized even though the membrane potentials fluctuate because of noise [3]. The question in a feedforward network is, whether the timing of spikes within a layer becomes more synchronized or not as the spike packet propagates through a sequence of neural layers. Detailed analyses of the activity propagation in feedforward networks have shown that homogeneous feedforward networks with excitatory synapses have a stable spike synchrony propagation mode [4, 5, 6]. Neurons, however, are embedded in more structured networks with excitatory and inhibitory synapses. Thus, such network structure would generate inhomogeneous inputs to neurons and whether spike synchrony is stable is not a trivial issue.

One simple way to detect the synfire chain phenomena would be to record from several neurons and find significant repeated patterns. If a spike packet propagates through a feedforward network, a statistically significant number of spike pairs would be found that have fixed relative time lags (or inter-spike intervals (ISIs).) Such correlated activity has been experimentally observed in the anterior forebrain pathway of songbirds [7], in the prefrontal cortex of primates [8], both *in vivo* and *in vitro* [9], and in an artificially constructed network *in vitro* [10]. To generate fixed ISIs by spike packet propagation, the propagation speed of a spike packet must be constant over several trials. The speed depends on spike patterns as well as the structure of the network. Conventional homogeneous feedforward networks have only one stable spike pattern, namely a spatially uniform synchronized activity, but structured networks can generally produce spatially inhomogeneous spike patterns. In those networks, the relation between propagation speed and differences in the spike pattern is not well understood.

It is therefore an important problem to study a biologically realistic, structured network in the context of the synfire chain. Among suggested network structures, Mexican-Hat-type (MH) connectivity is one of the most widely accepted as being representative of connectivity in the cortex [11]. Studies of a feedforward network with the MH connectivity (FMH) have been reported [12]. In a FMH, a localized activity propagates through the network, and this network is preferable to a homogeneous feedforward network because it can transmit analog information regarding position [12], and both position and intensity [13]. However, no detailed analytical work on the structured synfire chain has been reported. In this paper, we use the Fokker-Planck equation to analyze the FMH. The method of the Fokker-Planck equation enables us to analyze the collective behavior of the membrane potentials in an

identical neural population [14, 15]. When it is applied to the synfire chain [5], the detailed analysis of the flow diagram, the effect of the membrane potential distribution on the spike packet evolution, and the interaction of spike packets is possible [5].

This paper thus examines the feedforward neural network model with Mexican-Hat-type connectivity. Our strategy is, first, to describe the evolution of firing states through order parameters, which allows us to measure the macroscopic quantity of the network. Second, we relate the input order parameters to the output ones through the Fokker-Planck equation. Finally, we analyze the evolution of spike packets with various shapes, and investigate stable firing patterns and their propagation speeds.

2 Model

We analyze the dynamics of a structured feedforward network composed of identical single compartment, Leaky Integrate-and-Fire (LIF) neurons. Each neuron is aligned in a ring neural layer, and projects its axon to the next neural layer with the Mexican-Hat-type connectivity (Fig.1). The input to one neuron generally includes both outputs from pre-synaptic neurons and a random noisy synaptic current from ongoing activity. If we assume that the thousands of synaptic background inputs that connect to one neuron are independent Poissonian, instantaneous synapse, and have small amplitude of post synaptic potential (PSP), we can approximate the sum of noisy background inputs as a Gaussian white noise fluctuating around the mean of the total noisy inputs. The membrane potential of a neuron at position θ at time t, which receives many random Poisson excitatory and inhibitory inputs, can be approximately described through a stochastic differential equation as follows:

$$C\frac{\mathrm{d}v(\theta,t)}{\mathrm{d}t} = I^{\alpha}_{\mathrm{in}}(\theta,t) - \frac{v(\theta,t)}{R} + \tilde{\mu} + D'\eta(t), \tag{1}$$

$$I^{\alpha}_{\mathrm{in}}(\theta,t) = \int_{-\pi}^{\pi}\frac{\mathrm{d}\theta'}{2\pi}W(\theta-\theta')r^{\alpha}(\theta',t), \tag{2}$$

$$r^{\alpha}(\theta,t) = \int_{-\infty}^{0}\mathrm{d}t' r(\theta,t-t')\alpha(t'), \tag{3}$$

$$W(\theta) = W_0 + W_1\cos(\theta), \tag{4}$$

where C is membrane capacitance, R is membrane resistance, $I^{\alpha}_{\mathrm{in}}(\theta,t)$ is the synaptic current to a neuron at position θ, $\tilde{\mu}$ is proportional to the mean of the total noisy input, and $\eta(t)$ is a Gaussian random variable with $\langle\eta(t)\rangle = 0$ and $\langle\eta(t)\eta(t')\rangle = \delta(t-t')$. Here, D' is the amplitude of Gaussian noise. The input current $I^{\alpha}_{\mathrm{in}}(\theta,t)$ is obtained from the weighted sum of output currents $r^{\alpha}(\theta,t)$ generated by pre-synaptic neurons. The synaptic current is derived from the convolution of its firing rate $r(\theta,t)$ with the PSP time course $\alpha(t)$. Here, $\alpha(t) = \beta\alpha^2 t\exp(-\alpha t)$ where β is chosen such that a single EPSP generates a 0.0014 mV elevation from the resting potential. The Mexican-Hat-type connectivity consists of a uniform term W_0 and a spatial modulation term $W_1\cos(\theta)$. We set the reset potential and threshold potential as V_0 and V_{th}, respectively. We start simulations from stationary distribution of membrane potentials. The input to the initial layer is formulated in terms of the firing rate on the virtual pre-synaptic layer,

$$r(\theta,t) = \frac{r_0 + r_1\cos(\theta)}{\sqrt{2\pi\sigma^2}}\exp(-\frac{(t-\bar{t})^2}{2\sigma^2}), \tag{5}$$

where r_0 and r_1 are input parameters, and the temporal profile of activity is assumed to be the Gaussian with $\sigma = 1$ and $\bar{t} = 10$. Throughout this paper, parameter values are given as follows: $C = 100$ pF, $R = 100$ MΩ, $V_{\mathrm{th}} = 15$ mV, $D' = 100$, $\tilde{\mu} = 0.075$ pA, $V_0 = 0$ mV, $V_{\mathrm{th}} = 15$ mV, $\alpha = 2$, and $\beta = 0.00017$. Space is divided into 50 regions for the Fokker-Planck equation approach, and 10000 LIF neurons per layer are used in simulations.

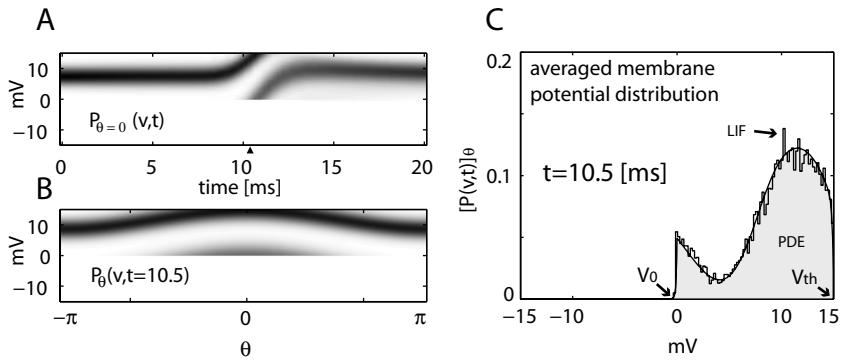

Figure 2: A: Dynamics of membrane potential distribution at $\theta = 0$. B: A snapshot of the membrane potential distributions for a range of $[-\pi \ \ \pi]$ at $t = 10.5$. C: A snapshot of the membrane potential distribution averaged with position θ. Results by a numerical simulation (LIF) and the Fokker-Planck equation (PDE) are shown.

3 Theory

The prerequisites for a full description of the network activity are time series of order parameters at an arbitrary time t defined as follows:

$$r_0(t) = \frac{1}{2\pi}\int \mathrm{d}\theta\, r(\theta,t), \qquad r_1(t) = \sqrt{(r_c(t))^2 + (r_s(t))^2}, \tag{6}$$

$$r_c(t) = \frac{1}{2\pi}\int \mathrm{d}\theta \cos(\theta) r(\theta,t), \qquad r_s(t) = \frac{1}{2\pi}\int \mathrm{d}\theta \sin(\theta) r(\theta,t), \tag{7}$$

where $r_0(t)$ is the population firing rate of the neuron population, and $r_c(t)$ and $r_s(t)$ are coefficients of the Fourier transformation of the spatial firing pattern which represent the spatial eccentricity of activity at time t. $r_c(t)$ and $r_s(t)$ depends on the position of the localized activity, but $r_1(t)$ does not. These order parameters play an important role in two ways. First, we can describe the input to the next layer neuron at θ in a closed form of order parameters. Second, their time integrals, which will be introduced later, become indices of the spike packet shape. Input currents are described with the order parameters as follows:

$$I^\alpha_{\mathrm{in}}(\theta,t) = W_0 r^\alpha_0(t) + W_1\left(r^\alpha_c(t)\cos(\theta) + r^\alpha_s(t)\sin(\theta)\right), \tag{8}$$

$$r^\alpha_{\{0,c,s\}}(t) = \int_{-\infty}^{0} \mathrm{d}t' \alpha(t')\, r_{\{0,c,s\}}(t-t'). \tag{9}$$

Given the time sequence of order parameters in the pre-synaptic layer, the order parameters in the post-synaptic layer are obtained through the following calculations. The analytical method we use here is the Fokker-Planck equation which describes the distribution of the membrane potential of a pool of identical neurons as the probability density $P_\theta(v,t)$ of voltage v at time t. The suffix θ denotes that this neuron population is located at position θ. We assume that there are a large number of neurons at position θ. Equation (1) is equivalent to the Fokker-Planck equation [16] within the limit of a large neuron number $N \to \infty$,

$$\frac{\partial}{\partial t}P_\theta(v,t) = \frac{\partial}{\partial v}J_\theta(v,t) + \delta(v-V_0)J_\theta(V_{\mathrm{th}},t), \tag{10}$$

$$J_\theta(v,t) = \left(\frac{v}{\tau} - \frac{I^\alpha_{\mathrm{in}}(\theta,t)+\tilde{\mu}}{C} + \frac{\partial}{\partial v}D\right)P_\theta(v,t), \tag{11}$$

where $J_\theta(v,t)$ is a probability flux and $D = \frac{1}{2}\left(\frac{D'}{C}\right)^2$. Boundary conditions are

$$P_\theta(V_{\rm th}, t) = 0, \tag{12}$$

$$r(\theta, t) = J_\theta(V_0^+, t) - J_\theta(V_0^-, t) = J_\theta(V_{\rm th}, t). \tag{13}$$

Equation (12) is the absorbing boundary condition at the threshold potential, and Eq. (13) is the current source at the reset potential. From Eq. (13), we obtain the firing rate of a post-synaptic neuron $r(\theta, t)$. The Fokker-Planck equations are solved based on the modified Chang-Cooper algorithm [17].

Figure 2 shows the actual distribution of the initial layer's membrane potentials and their dynamics which accepts virtual layer activity with parameter $r_0 = 500$ and $r_1 = 350$. Figure 2A shows the evolution of the probability density $P_{\theta=0}(v,t)$. From white to black, the probability becomes higher. Figure 2B is a snapshot of the probability density at time $t = 10.5$ over the region from $-\pi$ to π. As a result of a localized input injection, part of neuronal membrane potentials is strongly depolarized. The membrane potential distribution averaged over the neural layer is illustrated in Fig. 2C. It shows the consistency between the numerical simulations and the Fokker-Planck equations. The probability flow dropping out from the threshold potential $V_{\rm th}$ is a firing rate. Combined with these firing rates at each position θ and definitions of order parameters in Eqs. (6)-(7), the order parameters on the post-synaptic neural layer are again calculated. The closed forms of order parameters have been obtained.

Spatio-temporal patterns of firing rates and dynamics of order parameters in response to a localized input ($r_0 = 600, r_1 = 300$) and a uniform input ($r_0 = 900, r_1 = 0$) are shown in Fig. 3. When an input is spatially localized, the spatio-temporal firing pattern is localized with a slightly distorted shape (Fig. 3A). On the other hand, when a uniform input is applied, the spatio-temporal firing pattern is uniform as illustrated in Fig. 3B. We show an example of the time course of $r_0(t)$ and $r_1(t)$ in Fig. 3C and 3D for both the numerical simulation of $10,000$ LIF neurons and the Fokker-Planck equation. Elevation of time course of $r_1(t)$ in Fig. 3C indicates the localized firing. In contrast, the uniform input generates no response in $r_1(t)$ parameter as illustrated in Fig. 3D.

To quantitatively evaluate the spike packet shape and propagation speed, we define indices r_0, r_1, and σ. r_0 and r_1 can be directly defined as

$$r_0 = \int {\rm d}t\, r_0(t) - \text{spontaneous firing rate}, \quad r_1 = \int {\rm d}t\, r_1(t). \tag{14}$$

r_0 corresponds to the total population activity, and r_1 corresponds to spatial eccentricity of the activity. r_0 and r_1 are a natural extension of an index used in the study of the synfire chain [4] in the sense that an index corresponds to the area of a time varying parameters of the system, such as the population firing rate ($r_0(t)$) above the spontaneous firing rate, or spatial eccentricity ($r_1(t)$). The basic idea of characterizing the spike packet was to approximate the firing rate curve through a Gaussian function [4] as in Eq. (5). Here, the approximated Gaussian curve is obtained by minimizing the mean squared error with $r_0(t)$ and the Gaussian. We also use the index σ obtained from the variance of the Gaussian, and $\bar{t}$ as an index for the arrival time of the spike synchrony taken from the peak time of the Gaussian (Fig. 3C).

4 Results

Our observation of the activities of the FMH with various parameter sets reveals two types of stable spike packets. Figure 4 shows the activity of the FMH with four characteristic parameter sets of W_0 and W_1. Here we use $r_0 = 500$ and $r_1 = 350$ for the upper figures

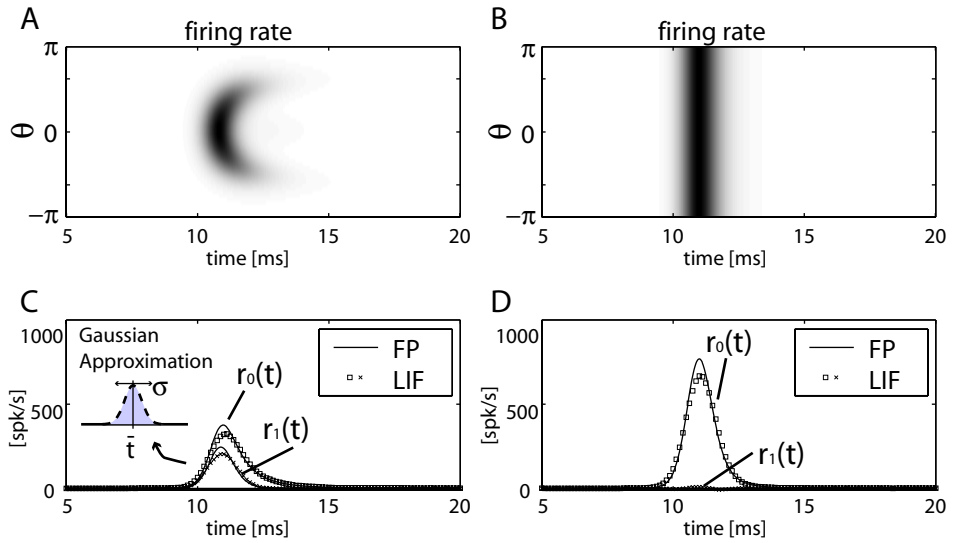

Figure 3: Activity profiles in response to a localized input (A,C) and a uniform input (B,D). A,B: Spatio-temporal pattern of the firing rates from neurons at position $-\pi$ to π. C,D: Time courses of order parameters $(r_0(t), r_1(t))$ calculated from numerical simulations of a population of LIF neurons (squares and crosses) and the Fokker-Planck equation (solid lines). The time course of order parameters in response to a single stimulus is approximated by using a Gaussian function. In C, Gaussian approximation of $r_0(t)$ is also shown. The variance of the Gaussian σ and the mean value $\bar{t}$ are used as the indices of a spike packet.

as a localized input and $r_0 = 900$ and $r_1 = 0$ for the lower ones as a uniform input. The common parameter is $\sigma = 1$ and $\bar{t} = 2$. When both W_0 and W_1 are small, no spike packet can propagate (Non-firing). When the uniform activation term W_0 is sufficiently strong, a uniform spike packet is stable (Uniform Activity). Note that even though the localized input elicits localized spike packets with several layers, it finally decays to the uniform spike packet. When the Mexican-Hat term W_1 is strong enough, only the localized spike packet is stable (Localized Activity). When W_0 and W_1 are balanced within a certain ratio, there exists a novel firing mode where both the uniform and the localized spike packet are stable depending on the initial layer input (Multi-stable). The results show that there are four types of phase and two types of spike packet in the FMH. The stability of a spike packet depends on W_0 and W_1. In addition, the difference of the arrival times of propagating spike packets in the 8th layer shown in the Multi-stable phase indicates that the propagation speed of spike packets might differ.

It is apparent that the propagation speed depends on the strength of the excitatory synapse efficacy, however, our results in the Multi-stable phase in Fig. 4 suggest that a spike pattern also determines the propagation speed. To investigate this effect, we plotted propagation time $\Delta\bar{t}$, the difference between propagation time $\bar{t}^{\rm post}$ and $\bar{t}^{\rm pre}$ for various W_1 (Fig. 5B). The speed is analyzed after the spike packet indices r_0, r_1 and σ have converged. The convergences of spike packets are shown in the flow diagram in Fig. 5A for $(W_0, W_1) = (1, 1.5)$ case. In Fig. 5B, each triangle indicates the speed of the localized activity, and each circle corresponds to that of the uniform activity. Within the plotted region ($W_1 = 1.4 \sim 2$), both the uniform and localized activities are stable, and no bursting activity is observed. This indicates that as W_1 rises the propagation speed of localized activity becomes higher. In contrast, the propagation speed of the uniform activity does not depends on W_1 because

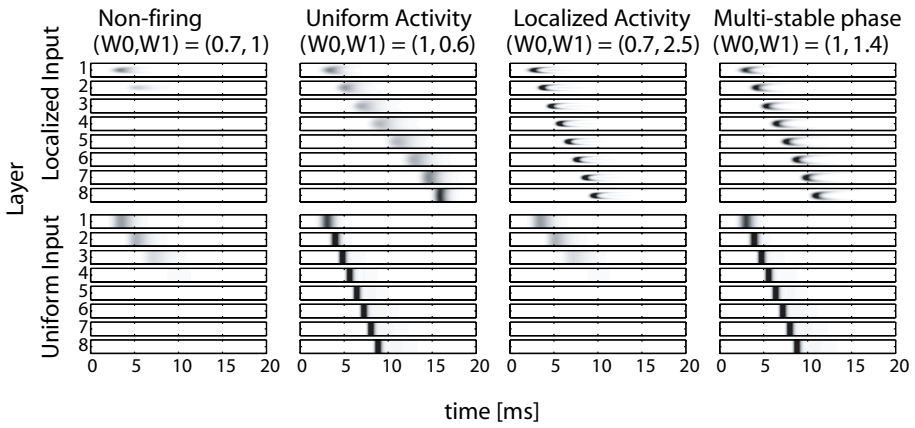

Figure 4: Four characteristic FMH with different stable states. The evolutions of firing rate propagation are shown. The upper row panels show the response to an identical localized pulse input, and the lower row panels show the response to a uniform pulse input.

uniform activity generates $r_c(t) = r_s(t) = 0$.

5 Summary

We have found that there are four phases in the $W_0 - W_1$ parameter space; Non-firing, Localized activity, Uniform activity, and Multi-stable phase. Multi-stable phase is the most intriguing in that an identical network has completely different firing modes in response to different initial inputs. In this phase, the effect of spike pattern on the propagation speed of the spike packet can be directly studied. By the analysis of the Fokker-Planck equation, we found that the propagation speed depends on the distinct firing patterns in the same network. It implies that observation of repeated spike patterns requires an appropriately controlled input if the network structure produces a multi-stable state. The characteristic speed of the spike packet also suggests that the speed of information processing in the brain depends on the spiking pattern, or the representation of the information.

Acknowledgment

This study is partially supported by the Advanced and Innovational Research Program in Life Sciences, a Grant-in-Aid No. 15016023 for Scientific Research on Priority Areas (C) Advanced Brain Science Project, a Grand-in-Aid No. 14084212, from the Ministry of Education, Culture, Sports, Science, and Technology, the Japanese Government.

References

[1] C. M. Gray, P. König, A. K. Engel, and W. Singer, "Oscillatory responses in cat visual cortex exhibit inter-columnar synchronization which reflects global stimulus properties," *Nature*, vol. 338, pp. 334–337, 1989.

[2] M. Abeles, *Corticonics: neural circuits of the cerebral cortex*. Cambridge UP, 1991.

[3] Z. Mainen and T. Sejnowski, "Reliability of spike timing in neocortical neurons," *Science*, vol. 268, pp. 1503–1506, 1995.

[4] M. Diesmann, M.-O. Gewaltig, and A. Aertsen, "Stable propagation of synchronous spiking in cortical neural networks," *Nature*, vol. 402, pp. 529–533, 1999.

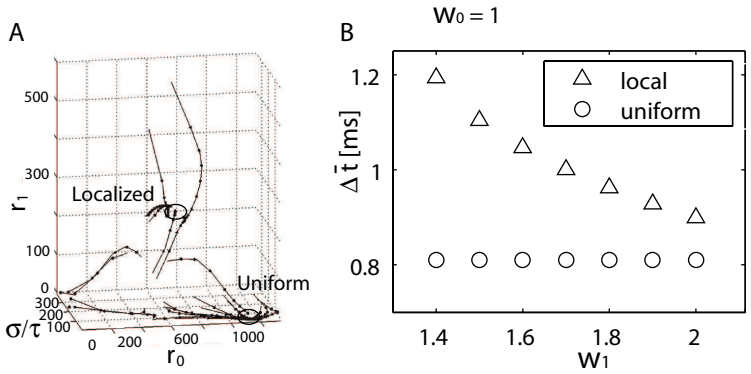

Figure 5: A: Flow diagram with parameter $(W_0, W_1) = (1, 1.5)$ where both localized and uniform spike packets are stable. Two attractors in high r_1 region (Localized) and high r_0 with $r_1 = 0$ region (Uniform) are shown. A sequence of arrows indicates the evolution of a spike packet in the $(r_0, \sigma/\tau, r_1)$ space. B: Plot of propagation time $\Delta\bar{t}$ that is necessary time for a spike packet to propagate one neural layer. These results indicate that localized spike packets propagate slower than the uniform ones.

[5] H. Câteau and T. Fukai, "Fokker-planck approach to the pulse packet propagation in synfi re chain," *Neural Networks*, vol. 14, pp. 675–685, 2001.

[6] W. M. Kistler and W. Gerstner, "Stable propagation of activity pulses in populations of spiking neurons," *Neural Comp.*, vol. 14, pp. 987–997, 2002.

[7] R. Kimpo, F. Theunissen, and A. Doupe, "Propagation of correlated activity through multiple stages of a neural circuit," *J. Neurosci.*, vol. 23, no. 13, pp. 5750–5761, 2003.

[8] M. Abeles, H. Bergman, E. Margalit, and E. Vaadia, "Spatiotemporal fi ring patterns in the frontal cortex of behaving monkeys," *J. Neurophysiol.*, vol. 70, pp. 1629–1638, 1993.

[9] Y. Ikegaya, G. Aaron, R. Cossart, D. Aronov, I. Lampl, D. Ferster, and R. Yuste, "Synfi re chains and cortical songs: Temporal modules of cortical activity," *Science*, vol. 304, pp. 559–564, 2004.

[10] A. Reyes, "Synchrony-dependent propagation of fi ring rate in iteratively constructed networks in vitro," *Nature Neuroscience*, vol. 6, pp. 593 – 599, 2003.

[11] D. H. Hubel and T. N. Wiesel, "Receptive fi elds, binocular interaction and functional architecture in the cat's visual cortex," *J. Physiol.*, vol. 160, pp. 106–154, 1962.

[12] M. C. W. van Rossum, G. G. Turrigiano, and S. B. Nelson, "Fast propagation of fi ring rates through layered networks of noisy neurons," *J. Neurosci.*, vol. 22, pp. 1956–1966, 2002.

[13] K. Hamaguchi and K. Aihara, "Quantitative information transfer through layers of spiking neurons connected by mexican-hat type connectivity," *Neurocomputing*, vol. 58-60, pp. 85–90, 2004.

[14] D. J. Amit and N. Brunel, "Dynamics of a recurrent network of spiking neurons before and following learning," *Network: Computation in Neural Systems*, vol. 8, no. 4, pp. 373–404, 1997.

[15] N. Brunel and V. Hakim, "Fast Global Oscillations in Networks of Integrate-and-Fire Neurons with Low Firing Rates," *Neural Comp.*, vol. 11, no. 7, pp. 1621–1671, 1999.

[16] H. Risken, *The Fokker-Planck Equation*. Springer-Verlag, 1996.

[17] J. S. Chang and G. Cooper, "A practical difference scheme for fokker-planck equations," *J. Comp. Phys.*, vol. 6, pp. 1–16, 1970.